SU-8 based Flexure-FET biosensor to achieve Ultra-sensitive Response

Durgesh Chaurasiya

A Dissertation Submitted to

Indian Institute of Technology Hyderabad

In Partial Fulfillment of the Requirements for

The Degree of Master of Technology

भारतीय प्रौद्योगिकी संस्थान हैदराबाद
Indian Institute of Technology Hyderabad

Department of Electrical Engineering

June, 2015

Declaration

I declare that this written submission represents my ideas in my own words, and where others' ideas or words have been included, I have adequately cited and referenced the original sources. I also declare that I have adhered to all principles of academic honesty and integrity and have not misrepresented or fabricated or falsified any idea/data/fact/source in my submission. I understand that any violation of the above will be a cause for disciplinary action by the Institute and can also evoke penal action from the sources that have thus not been properly cited, or from whom proper permission has not been taken when needed.

(Signature)

Durgesh Chaurasiya

EE12M1013

Approval Sheet

This thesis entitled "SU-8 Based Flexure-FET Biosensor to Achieve Ultra-Sensitive Response" by Durgesh Chaurasiya is approved for the degree of Master of Technology from IIT Hyderabad.

_____
External Examiner

Ch. Sobhanbabu

_____
Internal Examiner

_____
Adviser

_____
Co-Adviser

_____
Chairman

Acknowledgements

Dedicated to

My Family and friends………

Abstract

Recent advancements in nano-electronics have resulted in a new class of exciting devices such as Flexure-FET [1] (flexure sensitive field effect transistor). Flexure-FET is a potential candidate for detecting bio-molecules. Sensitivity of classical biosensors such as electrical [2] and mechanical [3] biosensors suffer from fundamental limitation. Sensitivity of electrical biosensors may be severely affected if the biomolecules to be detected are charge neutral. In addition, it also suffers from electrostatic screening due to presence of charged molecules in the solution. On the other hand, mechanical biosensors are afflicted by the complex scheme of optical setup to detect deflection of beam/cantilever, when beam captures the biomolecules. Moreover, its response is linear with change in mass and surface stress of beam/cantilever.

Flexure-FET utilizes the advantages of classical electrical and mechanical biosensors to give ultrasensitive response. Here, gate of FET is replaced with the fixed-fixed micro-beam. Micro-beam is biased near to pull-in instability (V_{pi}) and MOSFET channel is biased in sub threshold regime (V_t). This is done to operate both devices (MOSFET and micro-beam) in their non-linear regime simultaneously so that sensitivity is maximum. Flexure-FET is biased in sub-threshold regime below pull-in (i.e., $V_t \approx V_{pi}$). It is important to keep the pull-in potential of beam low, owing to the fact that low V_t MOSFETs can be operated at a higher speed (as V_{pi} of micro-beam and V_t of MOSFET should be approximately equal, implying that low V_{pi} will require design of a MOSFET having low V_t). Hence it necessitates the design and optimization of beam dimensions to have low stiffness, which in turn decides low value of V_{pi}. One of the key parameters to determine stiffness is the Young's modulus (E) of material. Furthermore simulation result shows that a material having the smallest young's modulus exhibits the lowest V_{pi} (Fig.1b).

We have chosen polySi ($E = 160$ GPa), gold ($E = 33{\sim}54$ GPa) and SU-8 ($E = 2{\sim}4.4$ GPa) as beam material and simulated the beam in real environment using Coventorware to compare their V_{pi}. Simulation results (Fig.1b) show that the SU-8 based beam exhibits the lowest V_{pi}. After selecting SU-8 as beam material, we optimized the dimensions of beam. After optimizing the beam dimensions using Coventorware, we modelled the FET whose V_t is near to V_{pi}. Multiphysics simulation of Flexure-FET is done using COMSOL. The adsorption of target bio-molecules causes mechanical deflection which is transduced as change in drain current of MOSFET. By simulations, we observed changed in drain current up to 4th order. (I_d before sensing = 1.1 pA and I_d after sensing = 17.3 nA.).

Contents

Chapter 1

Introduction

1.1 Classical Biosensors

Today, biosensors such as glucometer, lactate sensor, alcohol sensor etc, are becoming an integrated part of human beings. A biosensor is a device which takes a biomolecule as input and converts its response into measurable signal such as an electrical or mechanical signal, based on sensing mechanism.

Biosensor can also be divided into two components: Bio-receptor and transducer. Here, bio-receptor recognizes target biomolecules and attracts towards. Transducer converts this response into desirable/measurable signal.

We can classify biosensors broadly into two categories: 1. Electrical Biosensors and 2. Mechanical Biosensors. Electrical biosensors are one where electrical properties such as current or impedance/resistance changes due to proximity or contact with biomolecules in analyte. Examples of electrical biosensors are nanowire FET (Figure1), piezoelectric sensors etc.

Mechanical biosensors are one which use mechanical forces and motion to report the amount of analyte present in a sample. Most common and important example of such a device is the micro-cantilever (Figure2). It can be operated in two modes: 1. Static and 2. Dynamic mode. Capture of target biomolecules on cantilever surface modulates its mass stiffness and/or surface stress. This change in mechanical properties of cantilever can be observed as change in its resonance frequency (Dynamic mode), mechanical deflection or change in resistance of peizo resistive material (Static mode) attached to cantilever. In static mode, Micro-cantilever biosensors produce cantilever bending due to difference in the surface stress between upper and lower surface of cantilever. Deflection can be up or down depending on type of stress produced in beam (Compressive or tensile stress).
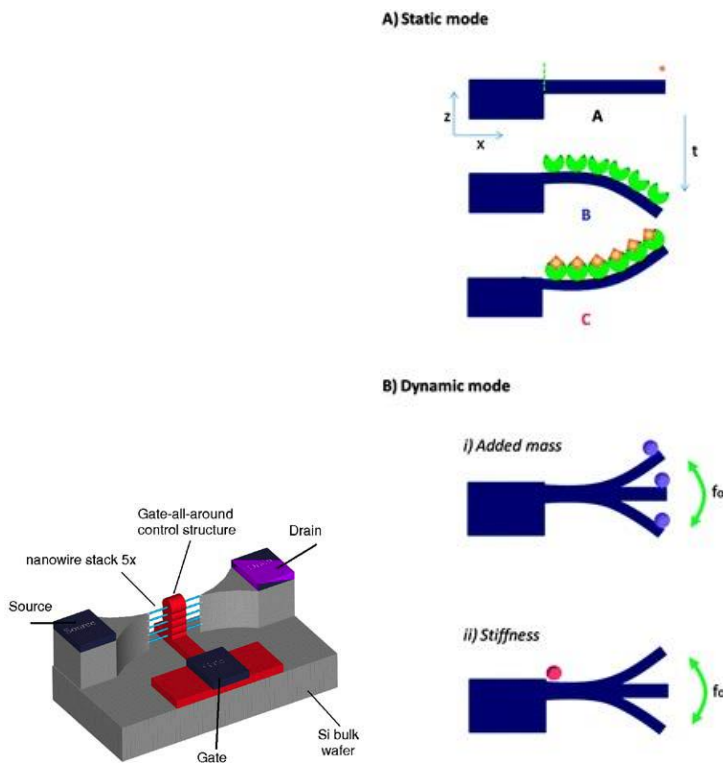
A) Static mode

B) Dynamic mode

i) Added mass

ii) Stiffness

Figure 1 Conceptual view of nanowire FET   **Figure 2 Microcantilever operational mode**

1.2 Fundamental Limitations of classical Biosensors

Sensitivity of classical biosensors such as electrical [2] and mechanical [3] biosensors suffer from fundamental limitations. Sensitivity of electrical biosensors may be severely affected if the biomolecules to be detected are charge neutral. So biomolecules to be detected using electrical biosensors must be electrically charged. In addition, it also suffers from electrostatic screening due to the presence of charged molecules in the solution.

On the other hand, sensitivity of mechanical biosensors aren't limited by charged neutral biomolecules or electrostatic screening effect. Rather they are afflicted by the complex scheme of optical setup necessary to detect deflection of beam/cantilever due to capturing of the biomolecules. When a biomolecule attaches with the functionalized beam, it changes the mechanical properties of the beam by modulating the mass, stiffness and/or surface stress of the beam. This change in the mechanical properties is detected by change in resonance frequency (dynamic mode operation of cantilever/beam) or change in deflection of beam or change in resistance of peizoelectric material(static mode) [4]-[5]. Moreover, its response is linear [6] or logarathmic [7]-[9] with change in mass and surface stress of beam/cantilever.

2

1.3 Motivation and Objective of Thesis

A nanoscale biosensors are widely regarded as potential candidate for ultrasensitive, label free detection of biochemical molecules. Our motivation to design an ultra-sensitive biosensors such that

- To detect biomolecules at very low concentration in analyte.
- Early stage detection of diseases like cancers.
- A low cost device.

1.4 Literature Survey

Recent advancement in nano-electronics have resulted in a new class of exciting devices such as Flexure-FET [1] (flexure sensitive field effect transistors). As Moore's law is expected to see an end, heterogeneous integration would be future of Microelectronics. Integration of MEMS, nanosensors etc. with traditional MOSFET help in realizing Biochips and Lab-on-a-chip devices. Flexure-FET is an excellent example of heterogeneously integrated device. It has been theoretically proven to be more sensitive biosensor than any other types of biosensor. Flexure-FET is potential candidate for detecting bio-molecules. It is regarded as ultrasensitive, label free detection of biomolecules. As we have already seen in section 1.2, classical biosensors suffer from fundamental limitations. So we need a methodology which can combine advantages of nanomechanical and electrical biosensors to give ultrasensitive response. Flexure-FET is one which combines advantages of both technolgies and doesn't suffer from their limitations. The sensing involves the static nano-mechanical response of the suspended gate or Flex-gate due to the adsorption of biomolecules. Nano-mechanical response can be generated either by neutral or charged biomolecules. The magnitude of nano-mechanical response could be attributed to the concentration of the target biomolecules in an analyte. The present day challenge is to detect even the lowest concentration of specific types of biomolecules which are usually so less in the early stages of diseases like Cancer. Using Flexure-FET even the smallest of the nano-mechanical response can be transduced to a significant change in an electrical signal and hence the lowest concentration of the target bio-molecules. At clinically threshold concentration of biomolecules, the change in free energy density on functionalized beam due to biomolecules was reported in range of 1 to 50 mJ/m^2 [10]-[13]. This change in free

energy density/surface stress (σ_s) is defined as integral of the normal stress or bulk stress (σ_m) in monolayer over its thickness:

$$\sigma_S = \int_0^{t_m} \sigma_m \, dz$$

1.5 Methodologies used to design Flexure-FET

To design Flexure-FET, we utilized following methodologies:

➢ Selection of MEMS Material suitable for improved sensitivity.

➢ Optimization of micro-beam parameters to improve the sensitivity.

➢ Design of MOSFET.

➢ Multiphysics coupling of fixed-fixed micro-beam and MOSFET.

1.6 Thesis Outline

Chapter 1: Is the introduction describing the motivation behind the work, literature survey and objective of the present work.

Chapter 2: Describes issues related to selection of material for micro-beam and criteria used to optimize the beam so that we can achieve very low pull-I potential.

Chapter 3: Describes basics of long channel MOSFET and modification in classical MOSFET to implement the Flexure-FET.

Chapter 4: Describes how we have done electromechanical coupling of MOSFET and micro-beam to analyze its response.

Chapter 5: Describes steps used for fabricating the Flexure-FET.

Chapter 6: Presents the conclusion to the thesis as well as future directions of this work.

Chapter 2

Analysis of MEMS Material and Optimization of micro-beam

2.1   Objective of analysing MEMS material for improved sensitivity

Flexure-FET utilizes the advantages of classical electrical and mechanical biosensors to give ultrasensitive response. Here, gate of FET is replaced with the fixed-fixed beam. Beam is biased near to pull-in instability (V_{pi}) and FET channel is biased in sub threshold regime (V_{th}). This is done to operate both devices (FET and micro-beam) in their non-linear regime simultaneously so that sensitivity is maximum. Flexure-FET is biased in sub-threshold regime below pull-in (i.e., $V_{th} \approx V_{pi}$). It is so because displacement of the fixed-fixed beam will be non-linear near to pull-in instability. In addition to this, drain current of FET is exponentially proportion to gate potential in subthreshold regime i.e. $I_d \propto \exp(V_{gs}\text{-}V_{th}/ mkT)$ where V_{gs} is gate to source potential, m= 1 + (C_{dm}/C_{ox}), C_{dm} is depletion capcitance and C_{ox} is gate oxide capacitance. Thus overall effect will be a highly non-linear change in drain current. It is important to keep the pull-in potential of beam low, owing to the fact that low Vth FETs can be operated at a higher speed (as V_{pi} of beam and V_{th} of FET should be approximately equal, implying that low V_{pi} will require design of a FET having low V_{th}). Hence it necessitates the design and optimization of beam dimensions to have low stiffness, which in turn decides low value of V_{pi}. One of the key parameters to determine stiffness is the Young's modulus (E) of material. Furthermore a material having the smallest young's modulus exhibits the lowest V_{pi}.

Thus, objective to select material for micro-beam is

> ➢ **Material which can easily be functionalized for target biomolecules.**
> ➢ **Material which can provide low value of pull-in potential V_{pi}.**

2.2   Result and discussion for selection of beam material

First challenge was to select suitable material for micro-beam for improved sensitivity. Materials used for analysis are gold (Au), PolySilicon and SU-8. Using these materials for

micro-beam, we simulated the beam Fig1(a) in real environment using Coventorware to compare their V_{pi}. Obtained result is shown in Fig1(b) and value of V_{pi} is listed in *Table1*. Simulation results show that the SU-8 based beam exhibits the lowest V_{pi}.
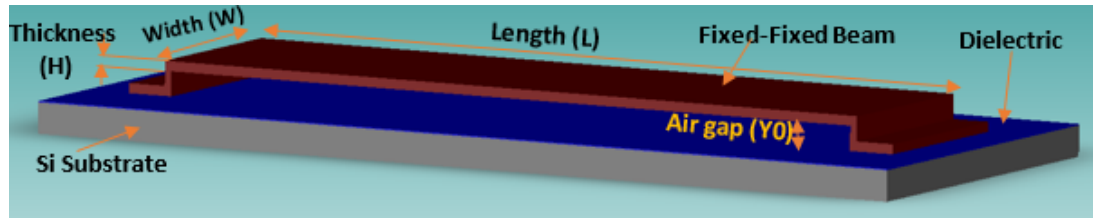
(a)
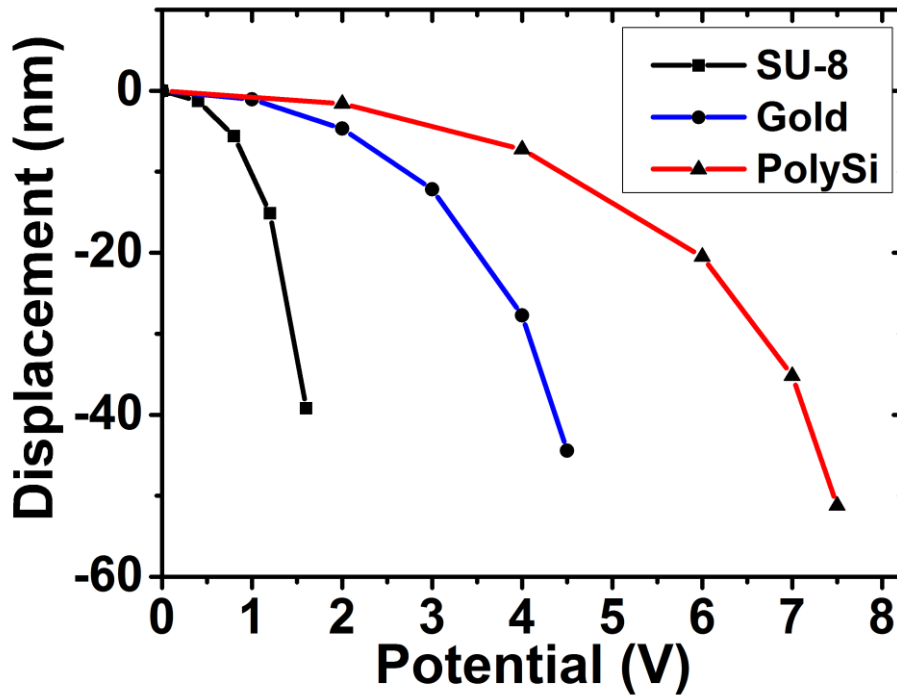
(b)

Figure 1(a) Beam model for pull-in comparison. Parameters of beam: L= 4 µm, W = 1 µm, H = 40 nm, Y0 = 100 nm and oxide thickness Tox = 10 nm. (b) Displacement of beam (Y) vs. Potential applied (V). Here we have changed the material of beam, and simulated it in Coventorware using PolySi,Au and SU-8, one at a time.

Table 1 : Pull-in potential

Material	E [GPa]	V_{pi} [V]
SU-8	2~4.4	1.75
Au	33~54	4.5
PolySi	160	7.5

2.3 Objective of optimizing the micro-beam parameters

To achieve beam having low value of stiffness, which in turn decides low value of pull-in potential V_{pi} which is ultimate aim of this thesis.

2.4 Optimization of the micro-beam parameters

After selecting beam material (SU-8), we had to optimize the beam dimensions to keep Vpi of beam as low as possible. For beam , stiffness is given by k = ($\alpha EWH3 / 12L3$) where α
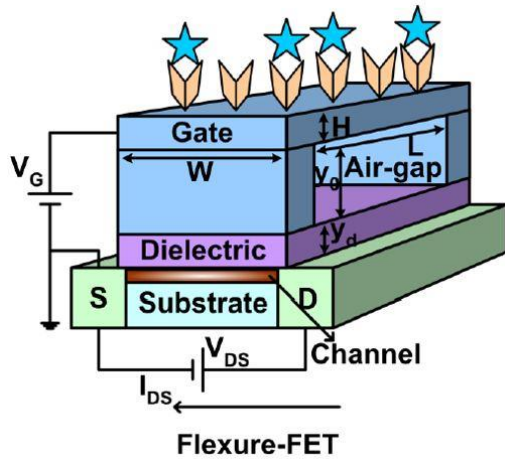

Figure 2 Flexure-FET

= 480 for fixed-fixed beam. Fig 3(a) and (b) show the variation of stiffness with respect to beam length by keeping beam thickness (h) and beam width (w) constant respectively. Fig 3 shows that as beam length increases by keeping other parameter constant , stiffness decreases by third power of L and becomes constant after a particular value of L. Fig 3(a) shows stiffness increses linearly with the width (W) of beam whereas in Fig3(b), stiffness increses by third power of beam thickness (H).

In Flexure-FET (Figure 2), length and width of beam will be along the width and chanel length of MOSFET respectively. Wider MOSFET lead to strong current but it increases the overall gate capcitance. This can lead to slow response of the device so we can't keep very long length of beam. From Fig 3(a), change in stiffness becomes negligible after L = 10 μm. So we chose beam length between 6 to 10 μm. We also observe that higher value of beam width increases the stiffness. As beam's width lies across the channel length of MOSFET , so lower value of width is desirable as It will lead to stronger current in MOSFET. So we chose beam's width w = 1μm.

   Fig3(b) shows that as film thickness of beam increases its stiffness increases too. So we have to choose lower value of beam thickness. We choose beam thickness between 250-500

nm. Thus, we chose final values of beam dimensions which is listed in *Table 2*. Air gap (Y_0) also plays a vital role to decide the pull-in potential of beam. As SU-8 is an insulator so we used very thin layer of gold (thickness of gold = 10 nm) as electrode for beam contact. We simulated this fixed-fixed beam (Fig1a). During simulation we observed that higher the value of air gap , larger the Vpi. For dimensions , listed in *Table 2*, we obtained $V_{pi} = 6.2$ V.
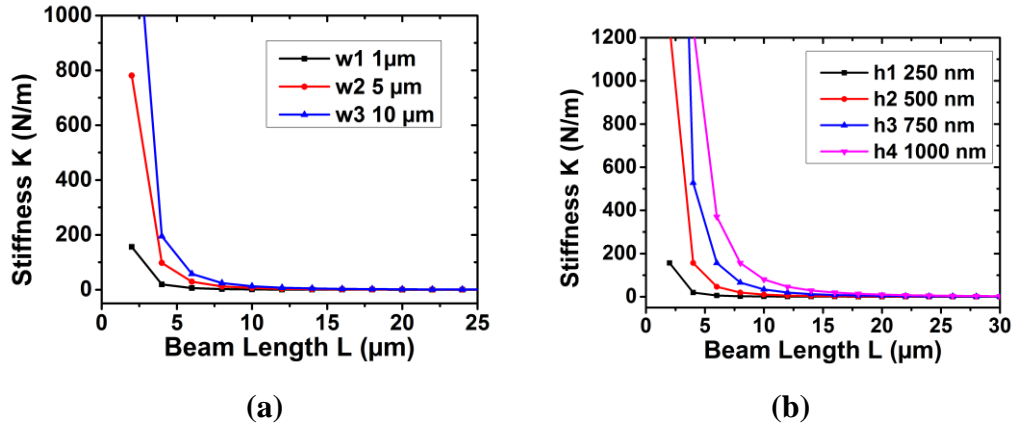

(a)   **(b)**

Figure 3 (a) Stiffness (k) vs. Beam Length (L) : h = 250 nm. (b) Stiffness (k) vs. Beam Length (L): w = 1 µm. Here we have chosen Young's modulus of SU-8 E=2 GPa.

Table 2: Optimized beam dimensions

Parameter	Value	Description
L	8 [µm]	Beam length
W	1 [µm]	Beam width
H	250 [nm]	Beam thickness
E_t	10 [nm]	Gold electrode thickness
Y_0	100 [nm]	Air gap
T_{ox}	10 [nm]	Dielectric thickness

8

Chapter 3

Design of MOSFET

3.1   Classical Long Channel MOSFET

Band diagram of classical long channel MOSFET is shown in figure1. Classical equation for threshold potential is given by

$$V_{th} = Vf_b + 2\phi_f + (\sqrt{2\,\epsilon_s\,q\,Na\,(2\,\phi_f + Vs_b)\,})/C_{ox}$$
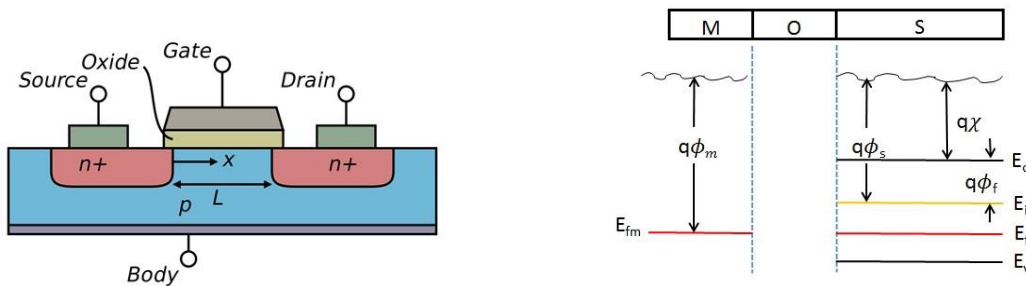
-----(1)

Figure 1 Cross sectional view of MOSFET and its band diagram

3.2   Modification in classical Equation of Vth for Flexure-FET

As gate of classical MOSFET is replaced by fixed-fixed micro-beam in Flexure-FET i.e. we have air gap between metal contact and oxide as shown in Figure 2.
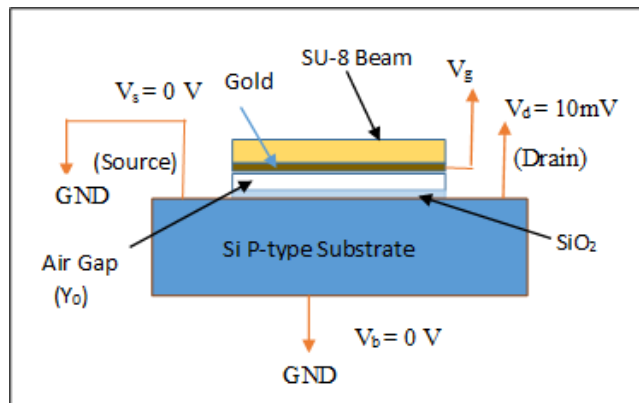
Figure 2 Cross sectional view of Flexure-FET

9

So C_{ox} in equation (1) neds to be replaced by capacitance due to oxide and air gap between Si and beam. So Classical equation of threshold potential is modified as

$$V_{th} = V_{fb} + 2\,\phi_f + (\sqrt{2\,\epsilon_s\,q\,Na\,(2\,\phi_f + Vsb)})/C \quad \text{------ (2)}$$

$$\text{Where } \left(\frac{1}{C}\right) = \left(\frac{1}{C_{air}}\right) + \left(\frac{1}{C_{ox}}\right)$$

$$V_{fb} = \phi_{ms} = \phi_m - \phi_s$$
$$\phi_s = \chi + \left(\frac{E_g}{2q}\right) + \phi_f$$
$$\phi_f = V_t \ln(Na/ni)$$

Metal work function= 5.1 eV , electron affinity = 4.05 , forbidden energy gap = 1.12 eV , intrinsic carrier concentration of Si = 1.5e10 [1/cm^3]. By subsituuting these values in above equations, we solved for N_a for different values of V_{th} in Matlab and then used the same in COMSOL. As in our design, we have obtained pull-in potential V_{pi} , equal to 6.2 V. As Vth ~ Vpi = 6.2 V. For this value of V_{th} , we obtained N_a=1.1e16 [1/cm^3]. All corresponding parameters are listed in *Table 3*. Corresponding I_d vs V_{gs} graph obtained in COMSOL simulation, is also shown in figure 3. Here, we can observe that V_{th} of dvice is 6.2 V.
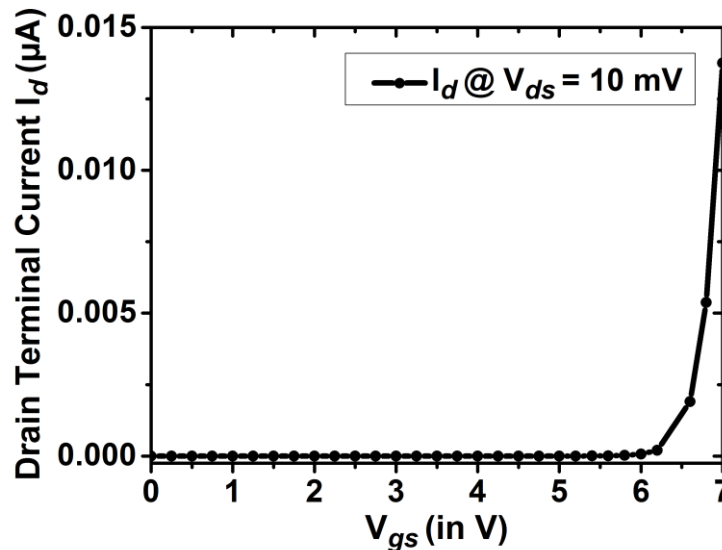

Figure 3 Id vs Vgs of MOSFET

3.3   Parameters of MOSFET to set required threshold potentials

As V_{pi} of beam structure is 6.2 V. So our target is to design a FET whose V_{th} is nearly equal to V_{pi}. Different parameters of MOSFET which sets its V_{th} = 6.2 V, are listed in *Table 3*. This structure Figure 2 is simulated in COMSOL multiphysics 4.4 and result in Figure 3 I_d vs. V_{gs} plot shows that V_{th} of FET is equal to 6.2 V.

Table 3 : MOSFET Parameter

Parameter	Value	Description
N_a	1.1e16[1/cm^3]	acceptor doping concentration
N_d	1e18[1/cm^3]	donor doping concentration of source/drain
T_{ox}	10 [nm]	gate oxide thickness
ε_{sio2}	4.5	dielectric constant of Insulator
φ_m	5.1 [eV]	metal work function

Chapter 4

Electromchanical Coupling of Micro-beam and MOSFET

4.1 Bulk Stress generated due to Biomolecules

At clinically threshold concentration of biomolecules , the change in free energy density on functionalized beam due to biomolecules were reported in range of 1 to 50 mJ/m2 [10]-[13]. This change in free energy density/surface stress (σs) is defined as integral of the normal stress or bulk stress (σm) in monolayer over its thickness:

$$\sigma_S = \int_0^{t_m} \sigma_m \, dz$$

--(1)

If we substitute the surface stress 1 to 50 mJ/m2 in equation(1), we get normal stress in monolayer (thickness ~ 20 nm) in range of 50 kPa – 2.5 MPa. This bulk stress value may vary with the different type of material used for beam. We applied these bulk stress values over the top of beam and observed the change in deflection of beam.

4.2 Electromechanical Coupling and Simulation Result discussion

Firstly, Figure 1 is simulated in COMSOL using electromechanics (emi) physics without bulk stress, which causes to deform the beam. We obtained the deformed beam as shown in Figure 2. Then this deformed beam is imported in semiconductor physics to calculate the drain current (say, I_{d1}).
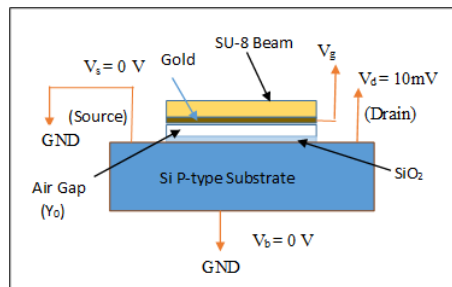
Figure 1 Cross sectional view of Flexure FET
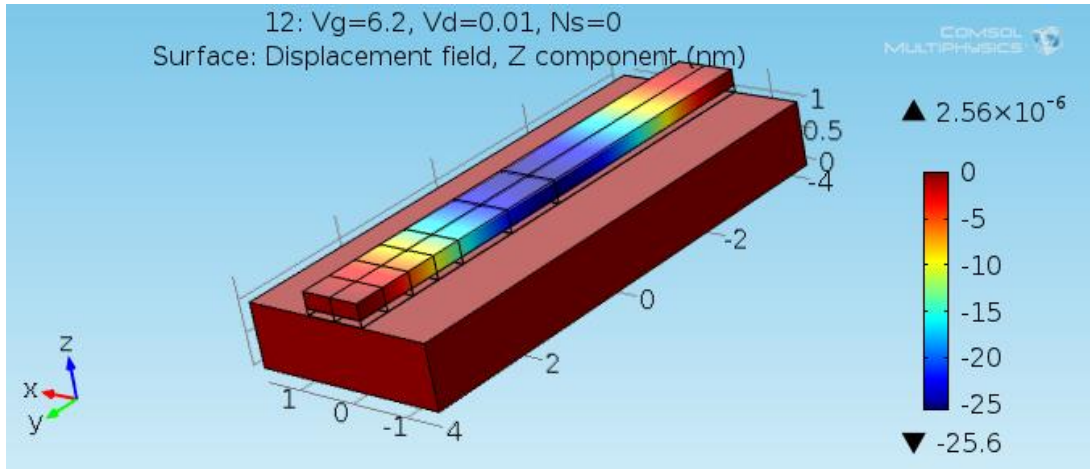
Figure 2 Deformed beam structure

Then we imported this deformed beam structure (Figure 2) into emi physics in COMSOL by applying bulk stress. We obtained the deformed beam as shown in Figure 3 and then imported this deformed beam in semiconductor physics to calculate the drain current (say , I_{d2}). This we performed over the range of bulk stress values and result (change in current ΔI_d = I_{d2}-I_{d1},where I_{d2} is drain current after deflectioon of beam due to attachment of biomolecules and I_{d1} is drain current before attachment of biomolecules) is shown in Figure 4.
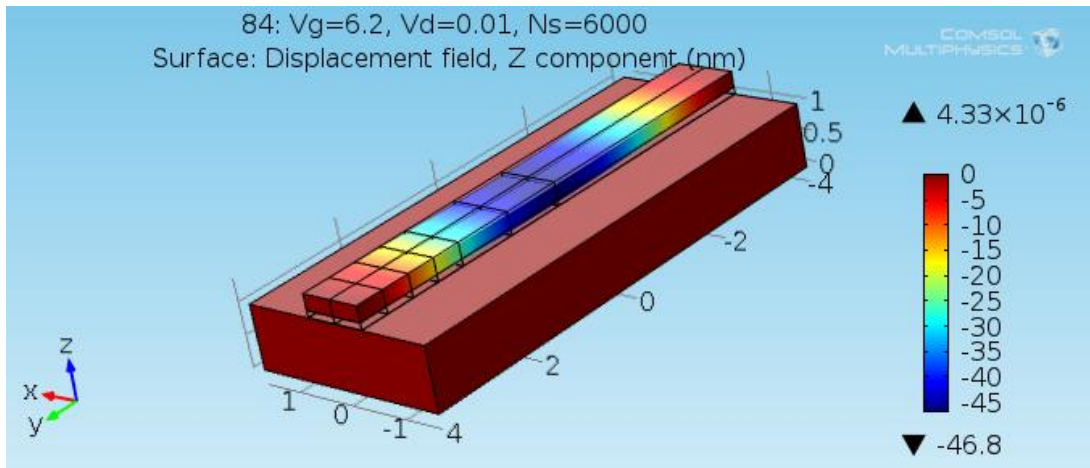
Figure 3 Deformation of beam after target biomolecules attaches with beam
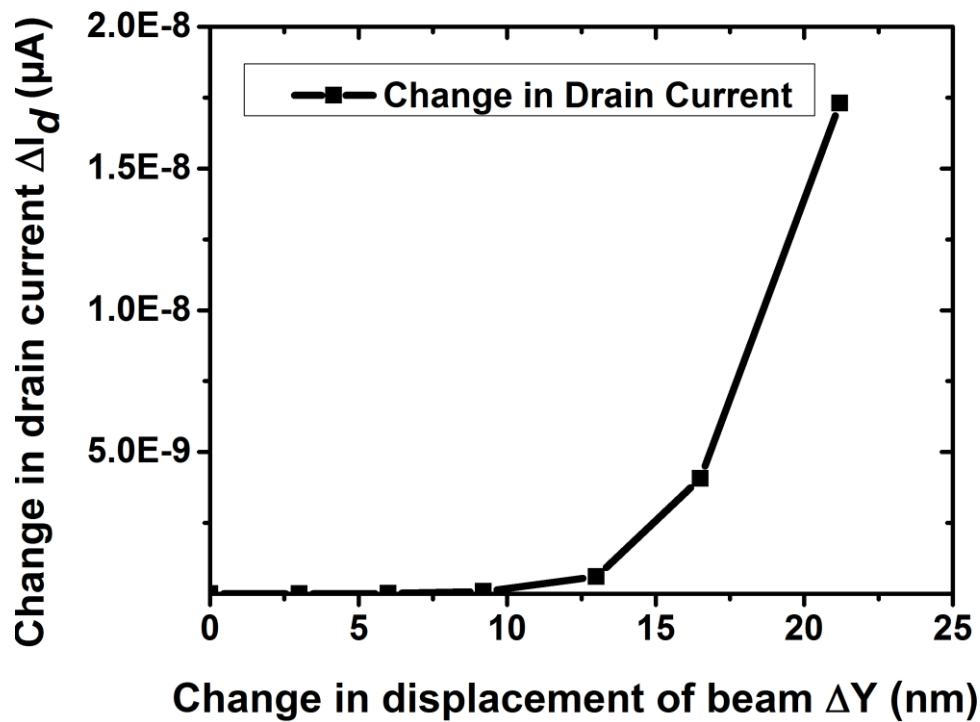
Figure 4 ΔI_d vs ΔY of the optimized beam used as gate of the FET. When SU-8 beam captures biomolecules, its stiffness changes which causes further displacement of beam from its equilibrium position at V_{pi} i.e. $\Delta Y = Y_0 - Y$.

Figure 6. shows that the non-linear deflection in beam due to biomolecules causes the change in potential of channel which results upto 4th order change in I_d of MOSFET i.e. I_d at equilibrium is 1.1 pA and due to biomolecules, I_d becomes 17.3 nA.

Chapter 5

Process steps to fabricate the Flexure-FET

5.1 Process steps to fabricate the flexure-FET

Using data obtained from simulation (Table 2 and Table 3 in chapter 3-4 respectively) below is process steps to fabricate the Flexure-FET.
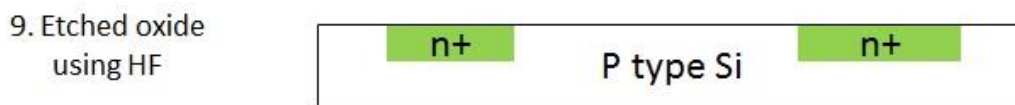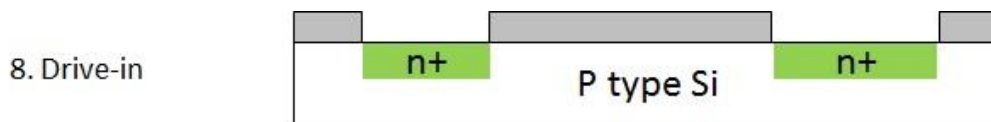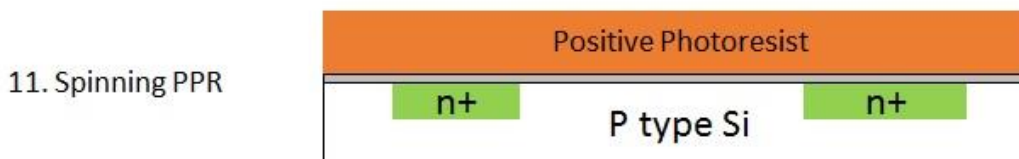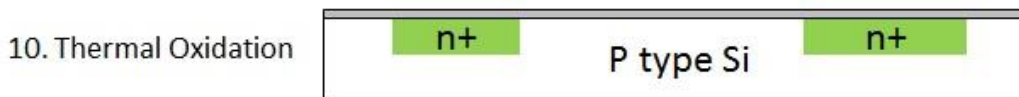
5. Removal of soft PPR

Positive Photoresist

P type Si

6. Etching off exposed Oxide and stripping off PPR

P type Si

7. Pre deposition

dopant gas

P type Si
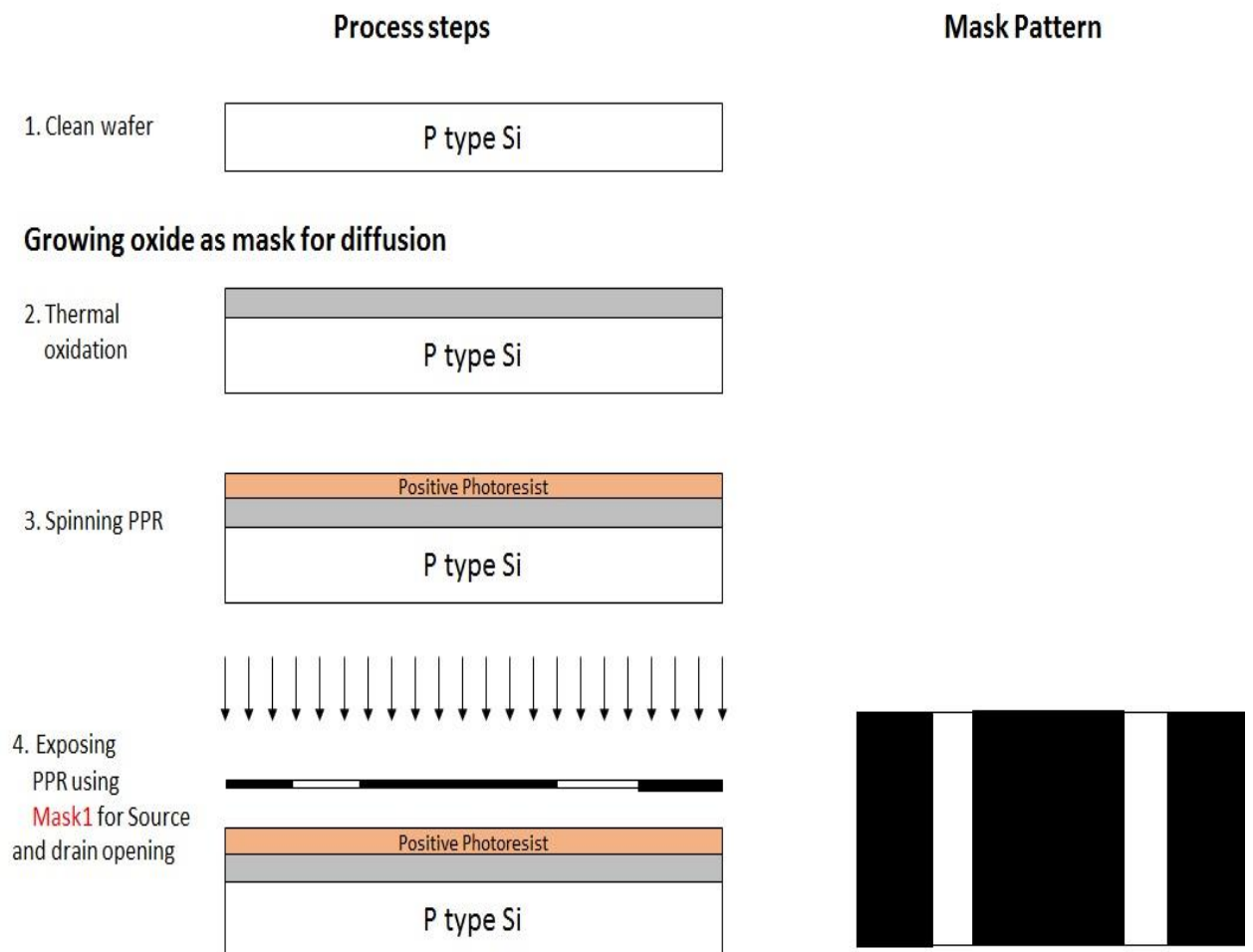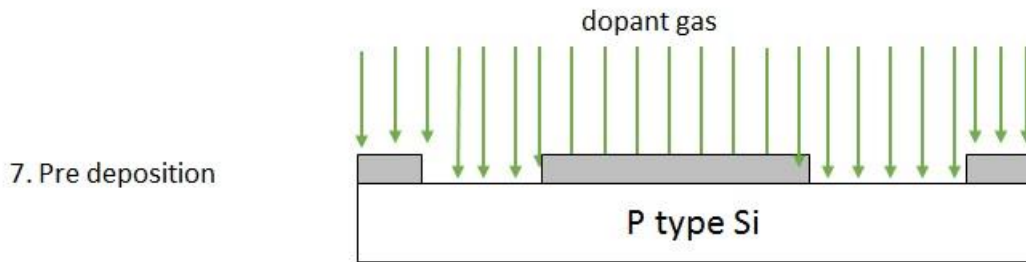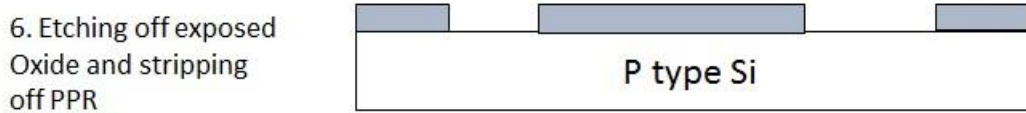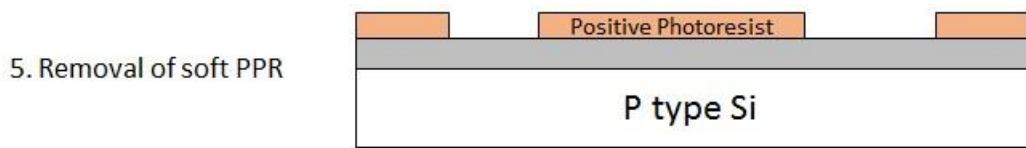
(a) Flow of dopant gases

P type Si
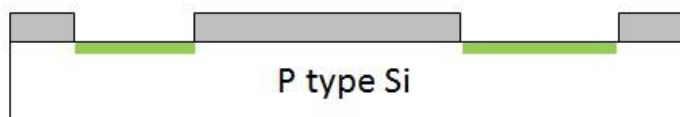
(b) After removal of dopant gases

8. Drive-in

n+   P type Si   n+

9. Etched oxide using HF

n+   P type Si   n+

Growing Gate oxide

10. Thermal Oxidation

n+   P type Si   n+

11. Spinning PPR

Positive Photoresist

n+   P type Si   n+

16

Process steps

Mask Pattern

12. Exposing PPR using **Mask1**

13. Removal of soft PPR

14. Etched oxide using HF

15. Stripped off PPR

Depositing Cu as sacrificial layer for air gap

Mask Pattern

16. Conformally depositing Cu for creating air gap

17. Spinning PPR

18. Exposing PPR using **Mask2**

Process steps   **Mask Pattern**

19. After patterning Cu

Depositing Ti for Gate , Source and Drain contact

20. Ti Deposition

21. Patterning Ti using
Mask 3

Gate

Source   Drain

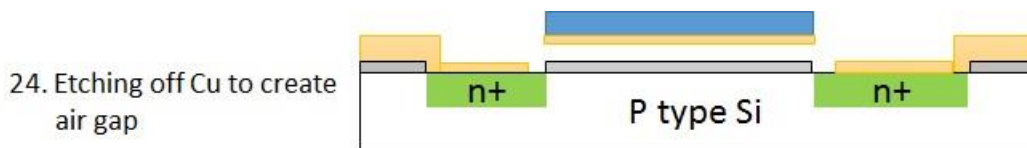**Forming SU-8 Beam**

22. SU-8 spinning for beam

23. Patterning SU-8 using
mask 4

24. Etching off Cu to create air gap

18
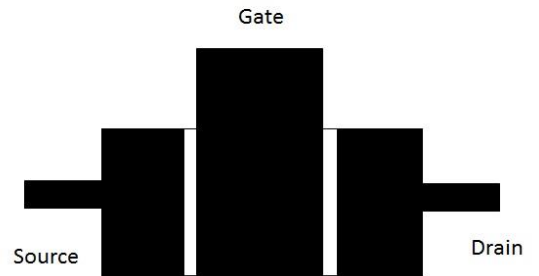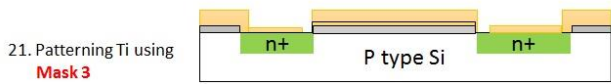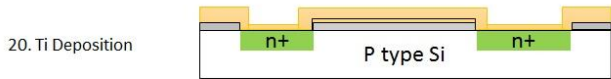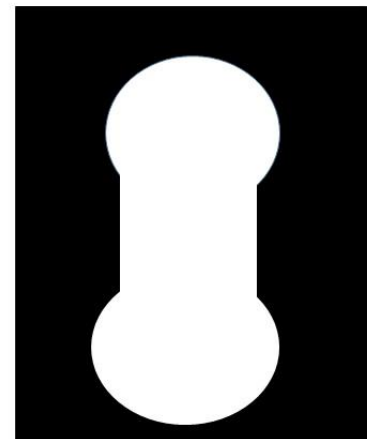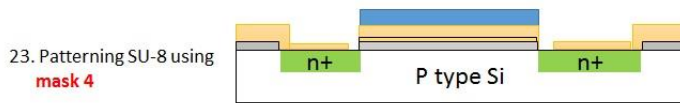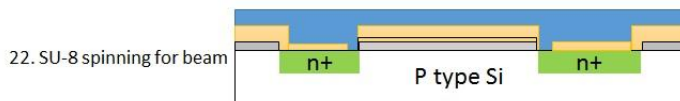
Chapter 6

Conclusion and Future work

6.1 Conclusion

Here, we demonstrated the Flexure-FET response using COMSOL Multiphysics 4.4. We observed that Flexure-FET can have a great outlook in biomedical field due to subtle change in drain current Id of FET. We proposed the optimized dimensions of micro-beam to fabricate the Flexure-FET.

6.2 Future work

Following works and improvements can be carried out in future as an extension of this work-

➢ We used gold as electrode for gate contact because SU-8 is insulator. If we can make SU-8 conductive then we can perform the same operation at much lower potential.

➢ Fabrication of Flexure-FET with proposed dimensions.

➢ If it is fabricated successfully then it can be useful for detection of many life threatening diseases like cancers at very early stage.

References

[1] Ankit Jain, Pradeep R. Nair, and Mohammad Alam , "Flexure-FET biosensor to break the fundamental sensitivity limits of nanobiosensors using nonlinear electromechanical coupling", PNAS 2012 109 (24) 9304-9308.

[2] P. Bergveld, "Thirty years of ISFETOLOGY: What happened in the past 30 years and what may happen in the next 30 years," Sensors and Actuators B: Chemical, Volume 88, Issue 1, 1 January 2003, Pages 1-20, ISSN 0925-4005.

[3] Arlett JL, Myers EB, Roukes ML, "Comparative advantages of mechanical biosensors" Nat Nanotechnol. 2011 Apr;6(4):203-15.

[4] Wee   K,   et   al.   (2005),   "Novel   electrical   detection   of label-free disease marker proteins using peizoresistive self-sensing micro-cantilevers" Biosens Bioelectron 20:1932–1938.

[5] Boisen A, Thundat T (2009), "Design & fabrication of cantilever array biosensors" Material Today 12:3238.

[6] Ekinci K, Roukes M (2005),"Nanoelectromechanical systems. Rev Sci Instrum" 76 (061101):1 –12.

[7] Wee K,et al. (2005), "Novel electrical detection of label-free disease marker proteins using piezoresistive self-sensing micro-cantilevers" Biosens Bioelectron 20:1932–1938.

[8] Wu G, et al. (2001), "Bioassay of prostate-specific antigen (PSA) using microcantilevers" , Nat Biotechnol 19:856–860.

[9] Zhang J, et al. (2006), "Rapid and label-free nanomechanical detection of biomarker transcripts in human RNA", Nat Nanotechnol 1:214–220.

[10] J. Fritz, M. K. Baller, H. P. Lang, H. Rothuizen, P. Vettiger, E. Meyer, H. -J. Güntherodt, C. Gerber, and J. K. Gimzewski, "Translating biomolecular recognition into nanomechanics," Science, vol. 228, pp. 316–318, 2000.

[11] G. Wu, H. Ji, K. Hansen, T. Thundat, R. Datar, R. Cote, M. F. Hagan, A. K. Chakraborty, and A. Majumdar, "Origin of nanomechanical cantilever motion generated from biomolecular interactions," in Proc. Nat. Acad. Sci., vol. 98, 2001a, pp. 1560–1564.

[12] G. Wu, R. Datar, K. Hansen, T. Thundat, R. Cote, and A. Majumdar, "Bioassay of prostate specific antigen (PSA) using microcantilevers," Nature Biotechnol., vol. 19, pp. 856–860, 2001b.

[13] K. Hansen, H. Ji, G. Wu, R. Datar, R. Cote, and A. Majumdar, "Cantilever-based optical deflection assay for discrimination of DNA singlenucleotide mismatches," Analyt. Chem., vol. 73, pp.1567–1571, 2001.